CL-150193 Received: March 9, 2015 | Accepted: March 31, 2015 | Web Released: April 9, 2015

Aldehyde-specific Quinazoline Ring-Closure for Highly Sensitive Fluorescent and Redox Formaldehyde Detection

Wei Huang, Fuxing Shen, and Dayu Wu*
Jiangsu Key Laboratory of Advanced Catalytic Material, School of Petrochemical Engineering,
Changzhou University, Changzhou, Jiangsu 213164, P. R. China

(E-mail: wudy@cczu.edu.cn)

Structurally tunable small signaling molecules have been specifically designed to probe-free formaldehyde concentrations as low as 0.1 ppm, establishing the utility of probing the exposure limit for safe human consumption according to the guidelines suggested by W.H.O. The substrate, 2-aminobenzoylhydrazide, fluorescent core skeleton was designed for the construction of diverse quinazoline compounds with combinatorial substituent-pending potentials via rapid condensation reactions with aldehyde groups. After identifying the fluorescent species by ^{1}H NMR and X-ray crystallography, we demonstrate that the fluorescent emission is substituent dependent and that, by simple structural variation, the fluorescence can be tunable through controlling internal charge transfer (ICT) within a dye platform. Finally, by introducing more electron-rich ferrocene into the substrate to further undermine the ICT process, we demonstrate highly sensitive formaldehyde sensing through dual signal output, including fluorescence and redox potential.

Small signaling molecules including the chromophore, fluorophore, and redox active toward specific functional groups, such as aldehyde, are crucial to molecular sensing and detection.[1–3] The controllable photophysical properties make these molecules ideal for both in situ and real-time studies. Quinazolines represent the most interesting group of heterocycles that contain a pyrimidine nucleus in their structure.[4–6] The interest in synthesis of their analogs was widely invoked by interesting biological and pharmaceutical activity including containment of inflammatory disorders such as osteoarthritis, inflammatory bowel syndrome, and neurodegenerative impairments.[7,8] However, the emissive properties concerning the quinazoline platforms were seldom reported.[9] Specifically, modulation of the electron-donating substituents on a quinazoline group affects both internal charge transfer (ICT) and emission color, as making this substituent more electron-rich results in ICT-blocked emission enhancement upon guest binding. We reasoned that anchoring a more electron-donating group on the quinazoline group would provide a tunable emissive and sensing platform.

Meanwhile, formaldehyde (HCHO), as a volatile organic compound (VOC) in the environment, has attracted emerging attention during the past few years in that HCHO exposure is of grave concern and brings about serious damage to life even at low concentrations.[10–12] Various analytical methods have been developed for the detection of formaldehyde in the past decades.[13,14] However, most of these techniques require expensive and bulky instrumentation with high power demand and well-trained operators. The up-to-now developed formaldehyde sensors, including film-technology-based sensors and nanostructured materials can only work in gaseous phase and require a high temperature (200–400 °C) to achieve optimum measurements.[15–19] Concerns over toxic exposure to formaldehyde provide motivation to explore new methods for monitoring aqueous HCHO in environmental samples. Additionally, despite the development of individual single-signaling sensors, multichannel signaling receptors have been rarely reported on formaldehyde binding.[20–25] As a result, developing new and practical multisignaling sensors for formaldehyde is still a challenge.

Herein, 2-aminobenzoylhydrazide (quantum yield, $\Phi = 0.3\%$) as a synthetic platform was introduced as a fluorescent signaling group that undergoes a "signal reduction" when reacted with aromatic aldehyde.[26] The condensation products (**1**, $\Phi = 0.07\%$) exhibit weak emission relative to the starting material. The mechanism for emission reduction is considered to be ICT. To further validate the fluorescence source, an electrophilic group, i.e. $-NO_2$, was introduced into the molecular skeleton, the synthetic species, **2** ($\Phi \approx 0$), whose emission continues to decrease in intensity. Parallel studies reveal that the introduction of a strong electrophilic group may give rise to an efficient intramolecular charge-transfer process.

The condensation between aromatic aldehydes and 2-aminobenzoylhydrazide has been reported to form 1,2-dihydroquinazoline in both polar as well as nonpolar solvents like methanol, acetonitrile, benzene, THF, and chloroform.[27,28] The initial hydrazone further undergoes an intramolecular nucleophilic addition across the azomethine group, involving a cyclic six-membered transition state leading to the formation of the quinazoline ring.[29] The cyclization involved in this type of reaction was proposed previously based on NMR studies.[30] We herein discovered that the pyrimidine nucleus can be systematically modulated via stepwise condensation starting from 2-aminobenzoylhydrazide when we attempted to systematically prepare the corresponding nitro-appending 1,2-dihydroquinazoline chromophore **2a**–**2f** (Scheme 1). Analysis by ^{1}H NMR spectroscopy demonstrated that the final products can be stepwise prepared to bear different substituent groups (for details, see Supporting Information). The discovery of this novel core skeleton was based on our original attempt at diversity-oriented synthetic development of a novel core skeleton.

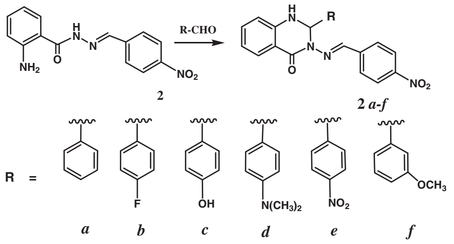

Scheme 1. The reaction between **2** and aromatic aldehyde to produce the corresponding quinazoline derivatives **2a**–**2f**.

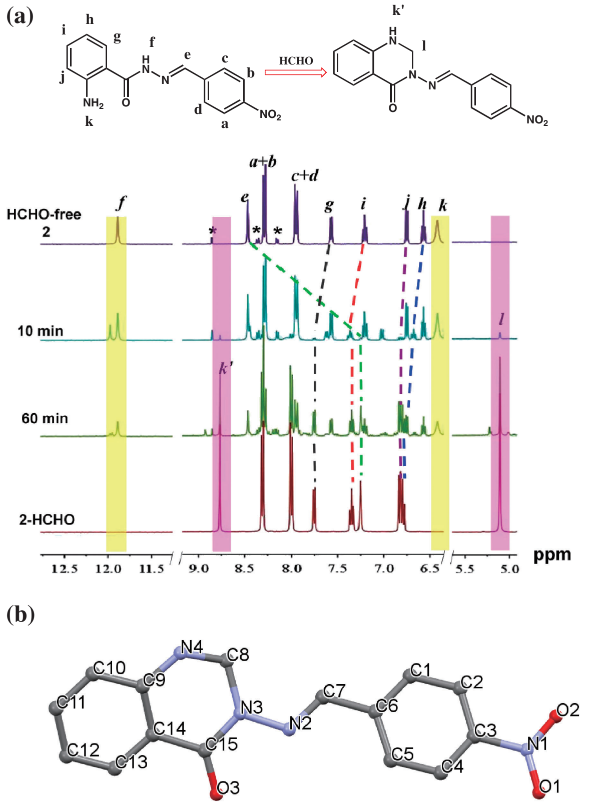

Figure 1. (a) ^{1}H NMR spectra of the reaction between **2** (16 mM) and formaldehyde solution (HCHO, 2 equiv) in DMSO-d_6 over time. **2** is highlighted in yellow, **2-HCHO** is highlighted in red, and chemical shifts are indicated in dotted lines. The asterisks represent trace amount of unidentified protons. (b) X-ray crystal structure of **2-HCHO**. For clarity, larger images are located in the Supporting Information. C: grey, N: blue, O: red.

As an application of the aldehyde-specific quinazoline ring-closure reaction, we extended the study to develop a monitoring reagent for the determination of aqueous HCHO in the near range from 0.1 to 1.0 ppm, because the recommended occupational exposure limit based on irritation is 1 ppm.[31] The Occupational and Safety Health Administration (OSHA) also established a short-term exposure limit of 2 ppm. Analysis by ^{1}H NMR titration spectroscopy of the congener **2** demonstrated that it can react with HCHO (180 min; room temperature) to yield a new species with the emergence of resonance (ppm) at 5.08 and 8.76. (Figure 1a). Meanwhile, the disappearance of resonance at 11.88 and 6.41 suggested that the condensation reaction occurs at both amine and imine sites. The presence of HCHO also causes significant downfield shifts of the H_g–H_h signals on the amine-appended benzene ring, indicative of the formation of a more conjugated structure. The ambiguity of the ^{1}H NMR spectra was further resolved by obtaining crystal structures of the HCHO condensation product, **2**-HCHO (Figure 1b).[32,33] Analysis of the structures unambiguously revealed that the reaction between **2** and HCHO yields a rigid, cyclic pyrimidine heterocycle. The C–N bond distance involving C9–N4 and C15–N3 is intermediate between that of a normal single bond and double one in the pyrimidine moieties of **2**-HCHO, indicative of the conjugation characteristic of the formed quinazoline.

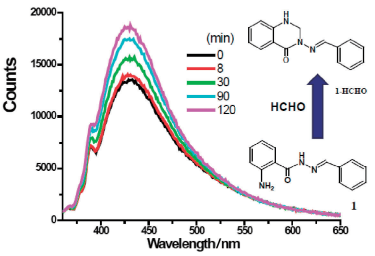

Figure 2. Emission spectra of **1** (1 μM) in acetonitrile at 0, 5, 10, 20, 40, and 80 min after the addition of 1 ppm formaldehyde.

To further examine the luminescent properties of **1** and **2** and their reaction with HCHO, the emission spectra were recorded before and after titration with a formaldehyde aqueous solution in acetonitrile. However, the analysis of complex **2** revealed negligible emission property and formaldehyde titration (1 ppm) could not arouse the obvious signal enhancement that is reminiscent of a system in which the ICT mechanism is operative. We then discovered that species **1** reacts with HCHO to yield the corresponding quinazolines (Figure 2). Compound **1** itself showed a weak emission maximum at 430 nm, while the titration of HCHO (1 ppm) into the solution of **1** aroused an increasing signal in intensity. Figure 2 indicates the typical time-dependent emission spectra of **1** after reaction with HCHO. Unfortunately, the titration of a lower concentration of HCHO, below 1 ppm, aroused negligible emission changes due to an unsatisfactory detection limit. However, these reagents quantitatively react with HCHO at room temperature and have a continuously increasing emissive signal due to the formation of rigid cyclization species, as revealed by ^{1}H NMR titration studies.

The crucial issue for formaldehyde detection is the lower detection limit. The World Health Organization (WHO) has set a standard of 0.08 ppm averaged over 30 min. According to these detection standards, a fast and highly sensitive sensor is desirable. Electron-rich ferrocene was anchored on the sensing platforms to suppress ICT and probe **3** ($\Phi = 0.12$) was obtained on purpose (Figure 3a). As expected, molecule **3** is sensitive enough to detect an environmentally relevant concentration of the HCHO molecule. Addition of 0.1 ppm of HCHO to an acetonitrile solution of **3** affords faster signal enhancement (2.5-fold in intensity over 120 min) than that of **1** with 1 ppm HCHO (1.3-fold, 120 min) (Figure 3b). Titration with a high concentration of methanol, acetone, and benzene (10 ppm) will not undermine the obvious intensity changes (Figure S12, Supporting Information). Other aldehyde compounds, i.e., acetaldehyde, were also tested to find aldehyde-group selective signal enhancement. LC-MS of the titration solution showed the main peak at 347.90 (cald. 347.19) and 359.90 (cald. 359.20) before and after HCHO titration, respectively, (Figure S14, Supporting Information) indicating the formation of HCHO-induced ring-closed products, 3-HCHO, as shown in Figure 3a.

Electrochemical sensing, in particular, is attractive from a practical standpoint because the signals can be easily read out on-site. Previous studies on complexation of ferrocene with binding ligands have shown that a positive shift of the Fe^{II}/Fe^{III} redox couple is observed.[34–36] Because the electron-rich cyclopentadienyl group is coplanar with the pyrimidine block, the electronic density within the ferrocene group is influenced by the HCHO-induced formation of more electronic conjugation along

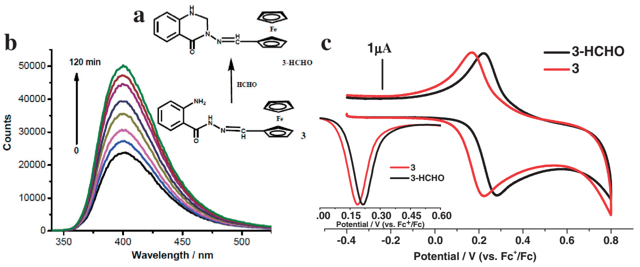

Figure 3. (a) Reaction scheme of substance **3** with HCHO. (b) Emission spectra of **3** (10 μM) with 15 min interval after the addition of 0.1 ppm HCHO over time. (c) CV in CH_3CN (10 μM) of free **3** (black) and upon titration of 1 ppm formaldehyde after 30 minutes (red). Inset is the corresponding DPV changes before and after addition of formaldehyde.

the –N–N– bridge. The amplified fluorogenical responses corresponding to the HCHO-induced conjugatation formation should be accompanied with a significant shift of the redox potential of the ferrocenyl group. As shown in Figure 3c, the cyclic voltammetric (CV) and differential pulse voltammetric (DPV) analyses of the substance **3** in an acetonitrile solution exhibit a quasi-reversible one-electron redox process around 190 mV vs. Fc^+/Fc. The addition of 1 ppm HCHO could induce a significant anodical shift of the ferrocene/ferrocenium redox couple of 60 and 32 mV in CV and DPV plots, respectively, over time. The linear relation between peak currents and the square root of the scan rates demonstrate that the diffusion-controlled process is dominant. (Figure S15)

In conclusion, we have shown that the quinazoline platforms can be structurally tunable toward highly sensitive detection of formaldehyde. This acyclic to cyclic "signal amplification" mechanism is unique, and we suggest that it is the origin of the excellent aldehyde selectivity observed at room temperature. We also demonstrate that the emission efficiency is easily modulated by making changes to the electron-donating ability in the conjugated backbone. Finally, signal transduction is optimized by systematically controlling intramolecular charge transfer, which affords enhanced fluorescence signals even in the presence of a low concentration of formaldehyde and enables an enhanced sensitivity during formaldehyde sensing to be achieved. This sensing scheme, while generic to aldehyde by the nature of its specific design and the key photophysical probing properties, might have application in both real-time sensing and array-based sensor strategies.

We thank the financial support by the Priority Academic Program Development of Jiangsu Higher Education Institutions (PAPD). This experiment work is financially funded by NSFC program (Nos. 21371010 and 21471023) and sponsored by Jiangsu Provincial QingLan Project.

Supporting Information is available electronically on J-STAGE.

References and Notes

1 D. J. Lloyd, D. J. St Jean, Jr., R. J. M. Kurzeja, R. C. Wahl, K. Michelsen, R. Cupples, M. Chen, J. Wu, G. Sivits, J. Helmering, R. Komorowski, K. S. Ashton, L. D. Pennington, C. Fotsch, M. Vazir, K. Chen, S. Chmait, J. Zhang, L. Liu, M. H. Norman, K. L. Andrews, M. D. Bartberger, G. Van, E. J. Galbreath, S. L. Vonderfecht, M. Wang, S. R. Jordan, M. M. Véniant, C. Hale, *Nature* **2013**, *504*, 437.
2 B. K. Wagner, H. A. Carrinski, Y.-H. Ahn, Y. K. Kim, T. J. Gilbert, D. A. Fomina, S. L. Schreiber, Y.-T. Chang, P. A. Clemons, *J. Am. Chem. Soc.* **2008**, *130*, 4208.
3 V. C.-L. Wong, H. L. Cash, J. Morse, S. Lu, A. Zhitkovich, *Cell Cycle* **2012**, *11*, 2526.
4 C. Shih, E. L. Fritzen, J. S. Swenton, *J. Org. Chem.* **1980**, *45*, 4462.
5 H. Nakamura, H. Yamamoto, *Chem. Commun.* **2002**, 1648.
6 G. Stájer, A. E. Szabó, P. Sohár, *Heterocycles* **1999**, *51*, 1849.
7 B. Jiang, S.-J. Tu, P. Kaur, W. Wever, G. Li, *J. Am. Chem. Soc.* **2009**, *131*, 11660.
8 Z. Chen, J. Chen, M. Liu, J. Ding, W. Gao, X. Huang, H. Wu, *J. Org. Chem.* **2013**, *78*, 11342.
9 a) S. Achelle, J. Rodríguez-López, F. Robin-le Guen, *J. Org. Chem.* **2014**, *79*, 7564. b) D. Liu, Z. Zhang, H. Zhang, Y. Wang, *Chem. Commun.* **2013**, *49*, 10001.
10 Y. Suzuki, N. Nakano, K. Suzuki, *Environ. Sci. Technol.* **2003**, *37*, 5695.
11 M. R. Ashmore, C. Dimitroulopoulou, *Atmos. Environ.* **2009**, *43*, 128.
12 N. Fiedler, R. Laumbach, K. Kelly-McNeil, P. Lioy, Z.-H. Fan, J. Zhang, J. Ottenweller, P. Ohman-Strickland, H. Kipen, *Environ. Health Perspect.* **2005**, *113*, 1542.
13 I. Castro-Hurtado, G. G. Mandayo, E. Castaño, *Thin Solid Films* **2013**, *548*, 665.
14 E.-X. Chen, H. Yang, J. Zhang, *Inorg. Chem.* **2014**, *53*, 5411.
15 X. Lai, D. Wang, N. Han, J. Du, J. Li, C. Xing, Y. Chen, X. Li, *Chem. Mater.* **2010**, *22*, 3033.
16 L. Zhang, J. Zhao, J. Zheng, L. Li, Z. Zhu, *Appl. Surf. Sci.* **2011**, *258*, 711.
17 L. Wang, J. Deng, T. Fei, T. Zhang, *Sens. Actuators, B* **2012**, *164*, 90.
18 P.-R. Chung, C.-T. Tzeng, M.-T. Ke, C.-Y. Lee, *Sensors (Basel Switzerland)* **2013**, *13*, 4468.
19 L. Xu, R. Xing, J. Song, W. Xu, H. Song, *J. Mater. Chem. C* **2013**, *1*, 2174.
20 K. Kawamura, K. Kerman, M. Fujihara, N. Nagatani, T. Hashiba, E. Tamiya, *Sens. Actuators, B* **2005**, *105*, 495.
21 N. Wang, X. Wang, Y. Jia, X. Li, J. Yu, B. Ding, *Carbohydr. Polym.* **2014**, *108*, 192.
22 R. Barik, S. K. Tripathy, M. Mohapatra, *J. Mater. Sci.* **2014**, *49*, 5345.
23 Q. Ma, H. Cui, X. Su, *Biosens. Bioelectron.* **2009**, *25*, 839.
24 H. Xie, C. Sheng, X. Chen, X. Wang, Z. Li, J. Zhou, *Sens. Actuators, B* **2012**, *168*, 34.
25 Q. Meng, T. Han, G. Wang, N. Zheng, C. Cao, S. Xie, *Sens. Actuators, B* **2014**, *196*, 238.
26 The absolute emission quantum efficiency was measured using the Edinburgh integrating sphere accessory following the De Mello method. See: J. C. de Mello, H. F. Wittmann, R. H. Friend, *Adv. Mater.* **1997**, *9*, 230.
27 R. S. Hoonur, B. R. Patil, D. S. Badiger, R. S. Vadavi, K. B. Gudasi, P. R. Dandawate, M. M. Ghaisas, S. B. Padhye, M. Nethaji, *Eur. J. Med. Chem.* **2010**, *45*, 2277.
28 D. Tinguiano, A. Sy, I. E. Thiam, M. Gaye, P. Retailleau, *Acta Crystallogr., Sect. E: Struct. Rep. Online* **2012**, *68*, 2374.
29 K. B. Gudasi, R. S. Vadavi, R. V. Shenoy, M. S. Patil, S. A. Patil, M. Nethaji, *Transition Met. Chem. (Weinh.)* **2005**, *30*, 661.
30 F. Fülöp, M. Simeonov, K. Pihlaja, *Tetrahedron* **1992**, *48*, 531.
31 D. Paustenbach, Y. Alarie, T. Kulle, N. Schachter, R. Smith, J. Swenberg, H. Witschi, S. B. Horowitz, *J. Toxicol. Environ. Health* **1997**, *50*, 217.
32 The light yellow crystals suitable for X-ray diffraction were obtained by slow diffusion of Et_2O vapor into the titration solution.
33 Crystallographic data for the structures in the form of CIF files have been deposited with the Cambridge Crystallographic Data Centre as supplementary publication No. CCDC 1038004. Copy of the data can be obtained free of charge via www.ccdc.cam.ac.uk/conts/retrieving.html or from the Cambridge Crystallographic Data Centre, 12, Union Road, Cambridge CB2 1EZ, UK (fax: (+44) 1223 336033; E-mail: deposit@ccdc.cam.ac.uk).
34 D. Wu, W. Huang, Z. Lin, C. Duan, C. He, S. Wu, D. Wang, *Inorg. Chem.* **2008**, *47*, 7190.
35 P. R. Singh, A. Q. Contractor, *Int. J. Environ. Anal. Chem.* **2005**, *85*, 831.
36 A. J. Tchinda, E. Ngameni, A. Walcarius, *Sens. Actuators, B* **2007**, *121*, 113.